IMPROVED CORE ANALYSIS MEASUREMENTS IN LOW PERMEABILITY TIGHT GAS FORMATIONS

S. Kryuchkov[1,2], J. Bryan[1,2], L.Yu[1], D. Burns[3] and A. Kantzas[1,2]
[1]PERM Inc., Calgary, Canada; [2]University of Calgary, Canada
[3]TAQA North Ltd, Calgary, Canada

This paper was prepared for presentation at the International Symposium of the Society of Core Analysts held in St. John's Newfoundland and Labrador, Canada, 16-21 August, 2015

ABSTRACT

Recovery of hydrocarbon gas in micro-Darcy rock is now becoming more common-place for gas producers. As part of the reservoir characterization associated with these systems, it is required to understand parameters such as the total porosity and permeability of the system, but also the initial water saturation and the effective gas permeability at this connate water saturation. This is still under the realm of what is termed "routine core analysis", but in these tight formations it is imperative to understand that these tests are actually very non-routine by nature. Current work presents a case study of core analysis that was run on plugs from a tight gas producing formation, and illustrates some of the pitfalls and corrections associated with measurements of this low permeability rock.

The case study combines low field NMR measurements with core flooding measurements of porosity and permeability. Cores are initially tested at their connate water saturations: NMR measures the initial water present in each core, and effective porosity and permeability to gas are measured through different core analysis techniques. By considering the time scales required for pressure to propagate within the cores, it is shown that "routine" measurement of permeability through multi-rate Darcy flow of gas is simply not adequate to properly characterize the core. Instead, core properties are measured through analysis of transient pressure data. Cores are then run through a Dean-Stark cleaning process, and NMR measurements are used to verify the ability of Dean-Stark to remove all water out of the cores. In this manner, post-cleaning measurements of porosity and permeability can be understood as effective values rather than their assumed absolute properties. This case study illustrates the challenges in making accurate measurements in micro-Darcy rock systems, and helps end-users to understand the dangers in using routine data without knowing how the data was collected.

INTRODUCTION

The objective of this test was to measure effective porosity and permeability in tight cores containing some residual water content. These values were then to be compared to measured porosity and permeability after attempting to clean water out of the cores. In order to assess the objective of this project, six core plugs from the Ferrier field operated by TAQA North Ltd. were cut from as received (pseudo-native-state) core and were sent

to PERM Inc. The field is a dry gas field with water present. The mineralogy is primarily carbonate.

The following work plan was defined at the start of the project:

- Measure dimensions of cores.
- Measure NMR spectra of initial cores with parameters of 0.16ms TE, 5000 Echoes, 12,000ms waiting time, and 128 trains.
- Measure pore volume and porosity with gas expansion and effective permeability to gas under 14.9MPag (2160psig) overburden pressure and near ambient pore pressure for the cores.
- Dean-Stark the cores, making sure to spend sufficient time to try to remove all water from the samples.
- Measure NMR spectra of cores after Dean Stark extraction with parameters of 0.16ms TE, 5000 Echoes, 2,000ms waiting time, and 128 trains.
- Measure pore volume and porosity with gas expansion and effective permeability to gas under 14.9MPag (2160psig) overburden pressure and near ambient pore pressure for the cores.
- Dual-energy CT scanning of the cores.

PROCEDURE

1) In order to execute the work plan, the following steps/modifications were carried out: Cut both ends of "as received" cores and obtain cylindrical plugs. The cylindrical plugs were thereafter named as "initial cores".
2) Re-measure dimensions and mass of initial cores.
3) Make up brine that is 125,000ppm (12.5%) of NaCl, and measure its density at 25°C. This is the expected salinity of the connate water in the cores.
4) NMR measurement of initial cores, as well a known amount of water to establish the amplitude index of the brine.
5) Place the cores under 14.9MPag (2160psig) overburden pressure and measure effective permeability to gas and porosity with gas expansion.
6) Again weigh the cores and measure NMR spectra of the cores after permeability and porosity measurement.
7) Dean-Stark the cores with Toluene for two weeks and then Acetone / Methanol for one week. Dry the cores in a conventional oven for 2 days at 105°C.
8) Take the mass of cores after extraction, and measure the NMR spectra of the cores.
9) Record the saturation values (S_w) before and after Dean-Stark extraction for all plugs.
10) Put the cores back to core holder under 14.9MPag (2160psig) overburden pressure and measure permeability to gas and porosity with gas expansion. Based on the post-cleaning NMR spectra, this step is either an absolute permeability or an effective permeability at lower water saturations.

Please note that the Dean Stark extraction had to be extended much longer than the standard method of 48 hours per solvent to ensure maximum contact of the solvents with

resident fluids. When comparing the results with routine core analysis measurements, care must be taken to reconcile the methodology used by the routine core analysis laboratory.

The porosity and permeability measurements were done following the methodologies of gas expansion and steady state permeability measurement. However, the results were analyzed with two different methods. One was the traditional approach. The second method relied on conducting a history matching of the pressure decay data as observed in the gas expansion method and by fitting different values of permeability until a match was found. The results were compared for all the plugs and all conditions.

Equations for the non-stationary gas flow are nonlinear, which calls for numerical solution for calculation of permeability. The total pressure change from initial state to final stationary state is used to characterize the porosity of the core.

The slope of the pressure curve as a function of square root of time at the origin depends on gas parameters, the geometry of the system, and the core porosity and permeability. This simplifies the formulation of the algorithm for finding permeability from the history match of the pressure decay data.

EXPERIMENTAL RESULTS AND DISCUSSION

Tested Core Properties

Tabulated values for all measured properties are included as well as sample graphs for individual plug measurements along with summary graphs that show trends.

Figure 1 shows the setup for porosity and permeability measurements. Tests were run at ambient temperature. Due to the relatively high permeability range measured in the core plugs (i.e. micro-Darcies compared to nano-Darcies expected for shale), pressure decay tests can be run relatively quickly and a more thorough temperature control was not considered necessary. In these small pore volume systems, the key to being able to measure pressure changes is to keep all dead volumes small, on the same order of magnitude as the pore volumes of the core. Traditional gas expansion core analysis equipment will not register an accurate change in pressure as gas enters the core, since the dead volumes are so much larger than that of the pores.

Table 1 summarizes the dimensions of each plug. The grain density numbers are estimated from bulk density and porosity calculations with liquid saturation included.

Table 2 summarizes the porosity and apparent permeability results for the “as received” cores. The term effective porosity refers to the porosity measured with gas expansion, i.e. the pore space that is saturated with gas only. The term total porosity is the sum of the gas saturated porosity (measured by gas expansion) and the liquid-filled porosity measured by NMR. Total porosity is then taken to be the sum of the gas expansion (effective) porosity and the bound water porosity, and fluid saturations are also calculated

on this basis. Without any additional information about the drilling mud used and the pressure conditions while drilling it is uncertain whether the determined liquid saturation values represent the true irreducible wetting saturation numbers; in the absence of any other data, the liquid in the core is assumed to be the saline brine present for this system (125,000 ppm salt).

Table 3 summarizes the porosity and apparent permeability results for the core after Dean Stark extraction. Despite the extended cleaning and drying there are still some notable amounts of liquid left in the core samples. This is due to the presence of small pores that hold water or solvent through capillary forces. In small pores the vapor pressure starts dropping because of the high curvature of the concave interfacial surfaces. This slows down the evaporation rate. In addition, surface area of pores with small radii is increasingly important, because of its relatively high contribution to the total surface area and because of the water films, which are hard to evaporate due to the surface forces.

Drying this remaining trapped water would require substantially higher temperatures for the cores to dry. This cannot be allowed because drying at extreme temperatures would damage the clays and the pore structure of the core would change. Thus the residual liquid volume has to be considered when the porosity is calculated. Once again, these liquid volumes are measured through NMR analysis of the cores; the effective porosity measured through gas expansion is still lower than the true porosity of the core. Estimates of total porosity are similar in Tables 2 and 3, indicating that this methodology is accurate.

The other significance of the remaining water saturation after cleaning is that the measured permeability values are not absolute permeability, but rather are still effective gas permeability measurements at some (albeit reduced) liquid saturation. Table 4 presents the apparent vs. Klinkenberg corrected permeability values for all plugs, all conditions for reference purposes. There is very little difference between apparent and Klinkenberg corrected permeability for the samples and pressure ranges tested here.

Discussion

Figure 2 shows a typical NMR spectrum for plug SP16A at the different stages of the experimental process. Figure 3 shows the effective porosity change before and after the Dean Stark extraction process. Figure 4 shows the total porosity before and after the extraction process. The fact that the total porosity measurements match is very encouraging and justifies the use of the NMR technology in compiling supplementary measurements even for routine purposes in the calculation of total porosity.

Figure 5 presents the permeability data before and after cleaning. An increase in permeability is seen for the cleaned core. Figure 6 presents rudimentary relative permeability curves for gas for different plugs lumped together based on their extrapolated absolute permeability values. It is fascinating that the data are lumped into three sets that can be fitted by straight lines. Extrapolation of these line to zero

permeability provides predictions for critical gas saturation that appears to be inversely proportional to permeability. In Figure 7 the permeability data are compared against the history matching predictions of the pressure transient data. The agreement is fairly good, although it becomes worse as the 1μD value is reached.

Figure 8 and Figure 9 show samples of the permeability measurements for plug SP16. They are presented as examples in order to illustrate the linearity of the steady state results. Note that routine core analysis will not be conducted under the steady state mode. For cores with permeability larger than 1μD, the steady state method remains the most reliable method for permeability measurement. However, the transient approach for cores with permeability below 1μD appears to be quite reliable.

Figure 10 and Figure 11 are examples of the pore volume measurement and the transient data used in the complex transient permeability predictions. The line in red is the pressure transient match if the steady state permeability is used and the black line is the permeability obtained by better history matching with permeability being the adjustable parameter.

As discussed above, the slopes of the pressure transient curves at short times are directly related to the permeability of the core and help to accelerate the history match procedure for permeability. Straight lines on the graph are trend lines based on few initial experimental and calculated points.

Some mismatch of the fitted curve and the observed pressures is due to the variation of the sample temperature during this experiment.

The combination of NMR and Dean Stark was very useful in calculating the saturations in the core. Table 5 summarizes the residual saturation after Dean Stark as calculated from mass balance and NMR. The agreement is good. It should be noted that there is no evidence of hydrocarbons in the reservoir (it is considered a dry gas reservoir).

However, the NMR could pick up the presence of residual hydrocarbons. Discriminating hydrocarbons from water in small pores and pore wedges or physically trapped in clay structures would require NMR with gradients. This can be done but it was not addressed in this paper.

Furthermore it should be noted that the reservoir cores were quite heterogeneous. Image examples of the different plugs are shown in Figure 12. The whole plugs are used for the testing under net overburden pressure. Thus core heterogeneity is maintained and it is utilized in the calculations.

PERM has developed numerous algorithms for the determination of special core analysis information from limited data through pore network modelling and pore level multi-physics programs [1-3]. This Digital Core Analysis approach would be ideal to provide

estimates of capillary pressures, resistivity indices, and relative permeability curves. The analysis can be extended to the utilization of NMR spectra as input [4]. However, this was deemed outside the scope of this project and will be pursued as future research.

CONCLUSIONS

- Deviations from routine methods (steady state testing) increase when permeability falls below the 1μD range.
- Transient methodology becomes more accurate and it can be used to measure permeability values below 1μD.
- The combined porosity measurements from gas expansion and NMR converge to the same total porosity value, irrespective of the saturation conditions of the core.

ACKNOWLEDGEMENTS

Funding of this project from TAQA North, as well as permission to publish this paper are gratefully appreciated.

REFERENCES

1. Ghomeshi, S., Bashtani, F., Bryan, J., Kryuchkov, S. and Kantzas, A. “Determination of Physical Properties of Tight Porous Media Using Digital Core Physics/Analysis”, accepted to Society of Core Analysis Symposium 2015, St. John's, NL, Canada, August 16-21, 2015.
2. Ghomeshi, S., Bashtani, F., Taheri, S., Skripkin, E., Kryuchkov, S., Bryan, J. and Kantzas, “Predicting Physical Properties of Porous Media at Sub-Pore Scales from Natural to Complex Heterogeneous Systems: Application in Tight Reservoirs”, GeoConvention 2015, Calgary, AB, Canada, May 4-8, 2015.
3. Rubin M., Wickens S., Leung S., Akinbobola O., Kent T. and Kantzas A. “Network Modeling and Two-Phase Flow in Tight Reservoirs” GeoConvention 2014, Calgary, Canada, 12–14 May 2014.
4. Talabi, O. and Blunt, M.J. “Pore-Scale Network Simulation of NMR Response in Two-Phase Flow”, *J. Pet. Sci. Eng.*, (2010), **72**, 1-9.

Table 1: Core ID and Dimensions

Sample ID	Depth (m)	Diameter (cm)	Length (cm)	Grain Density (kg/m^3)
SP16A	2565.70	3.81	6.05	2788.1
SP18A	2566.74	3.81	7.21	2779.4
SP19A	2567.70	3.81	7.53	2811.5
SP30A	2578.68	3.81	7.17	2750.8
SP33A	2580.30	3.81	7.27	2748.1
SP34A	2581.30	3.81	7.03	2992.1

Table 2: Initial Core Properties

Sample ID	Mass (g)	Effective Porosity (%)	Total Porosity (%)	k_{gas} (µD)		S_{liquid}	S_{gas}
				Steady state	Transient		
SP16A	175.68	5.57	10.62	0.81	2.07	0.48	0.52
SP18A	220.77	1.29	4.68	0.12	0.41	0.73	0.27
SP19A	226.34	3.75	7.70	0.09	0.89	0.51	0.49
SP30A	204.47	6.17	10.82	1.60	1.60	0.43	0.57
SP33A	210.82	4.84	9.18	2.36	2.36	0.47	0.53
SP34A	229.53	1.63	5.82	0.32	0.42	0.72	0.28

Table 3: Core Properties after Cleaning with Dean-Stark Extraction

Sample ID	Mass (g)	Effective Porosity (%)	Total Porosity (%)	k_{gas} (µD)			
				Steady state	Transient	S_{liquid}	S_{gas}
SP16A	172.82	10.10	10.59	6.71	7.56	0.05	0.95
SP18A	218.15	4.17	4.72	1.10	1.70	0.12	0.88
SP19A	222.99	7.42	7.92	1.03	1.84	0.06	0.94
SP30A	200.75	10.29	10.52	7.71	11.82	0.02	0.98
SP33A	207.41	8.86	9.26	12.51	13.60	0.04	0.96
SP34A	227.02	4.86	5.73	2.88	3.45	0.15	0.85

Table 4: Core Apparent and Klinkenberg Corrected Permeability Data

Sample ID	Before Cleaning (µD)		After Cleaning (µD)	
	k_g (µD)	k_∞ (µD)	k_g (µD)	k_∞ (µD)
SP16A	0.81	0.73	6.71	5.38
SP18A	0.12	0.10	1.10	0.91
SP19A	0.09	0.05	1.03	0.79
SP30A	1.60	1.59	7.71	6.54
SP33A	2.36	2.35	12.51	10.71
SP34A	0.32	0.29	2.88	2.52

k_∞ is Klinkenberg corrected permeability.

Table 5: Post Dean-Stark Water Mass Balance

Sample ID	Water Extracted (cm^3)	Residual water in core (cm^3)	NMR Residual water in core (cm^3)
SP16A	2.27	0.32	0.34
SP18A	1.68	0.53	0.45
SP19A	2.70	0.43	0.44
SP30A	3.17	0.17	0.19
SP33A	2.57	0.31	0.33
SP34A	1.62	0.71	0.70

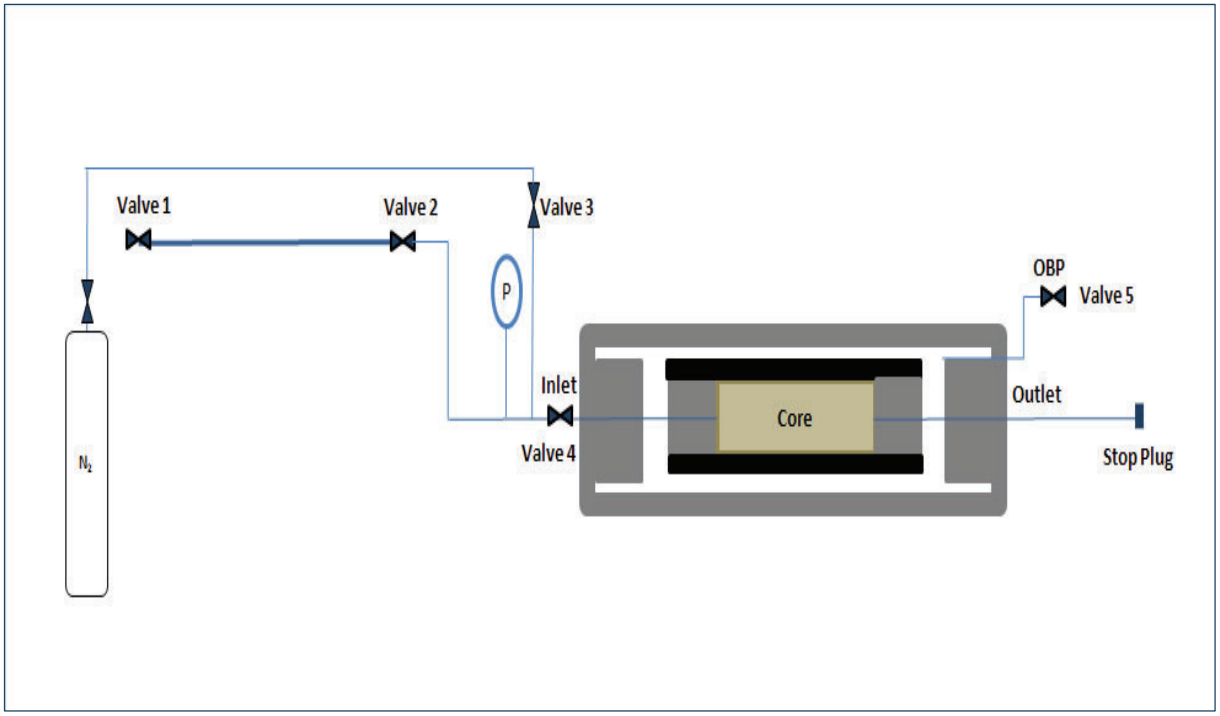

Figure 1: Core Testing Apparatus Rig Setup

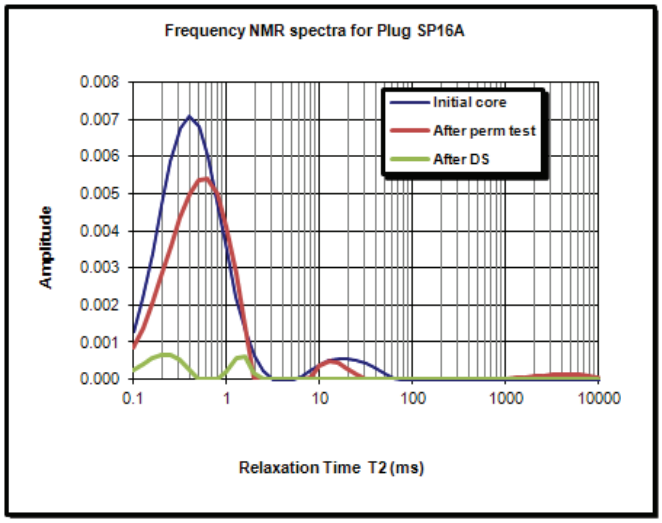

Figure 2: NMR Spectra for Plug SP16A

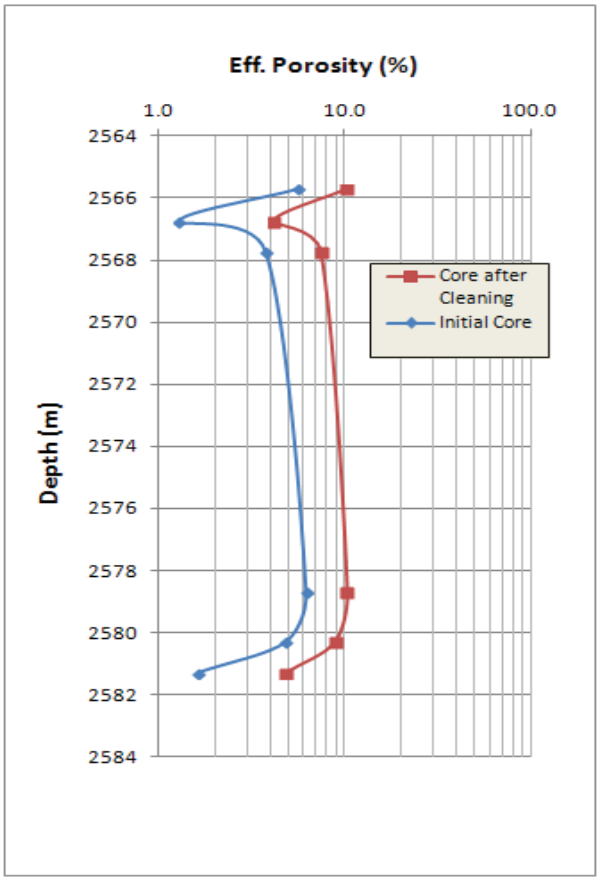

Figure 3: Effective Porosity of Initial Core and Core after Cleaning with Dean-Stark

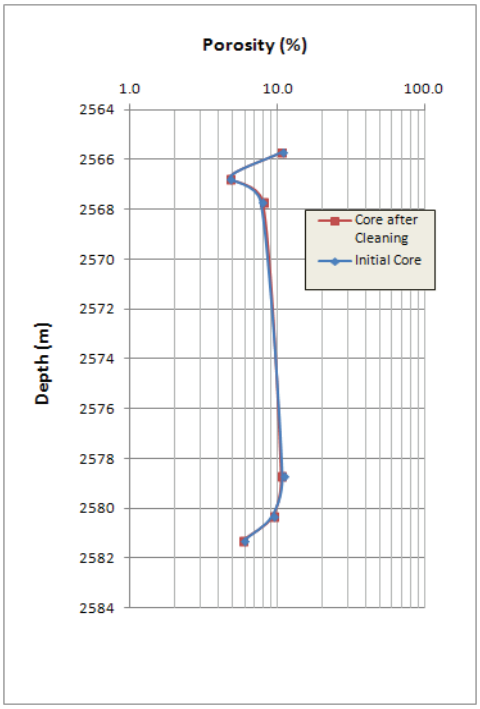

Figure 4: Total Porosity of Initial Core and Core after Cleaning with Dean-Stark

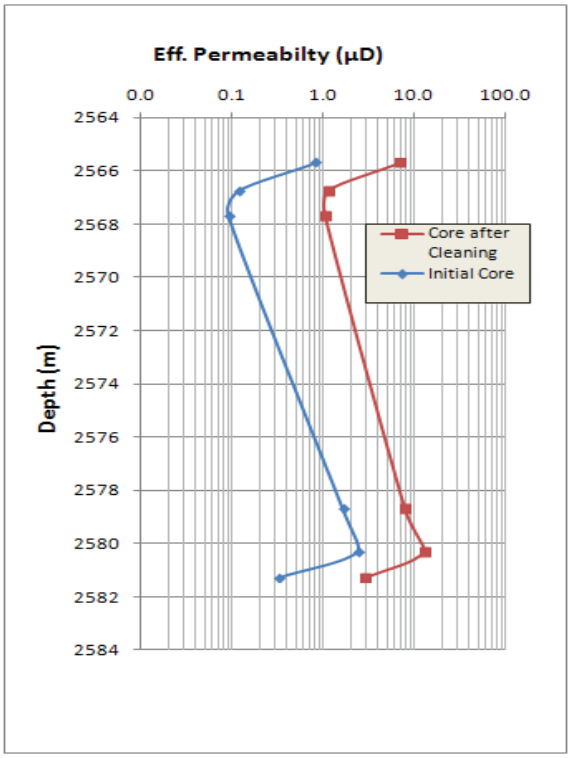

Figure 5: Gas Permeability of Initial Core and Core after Cleaning

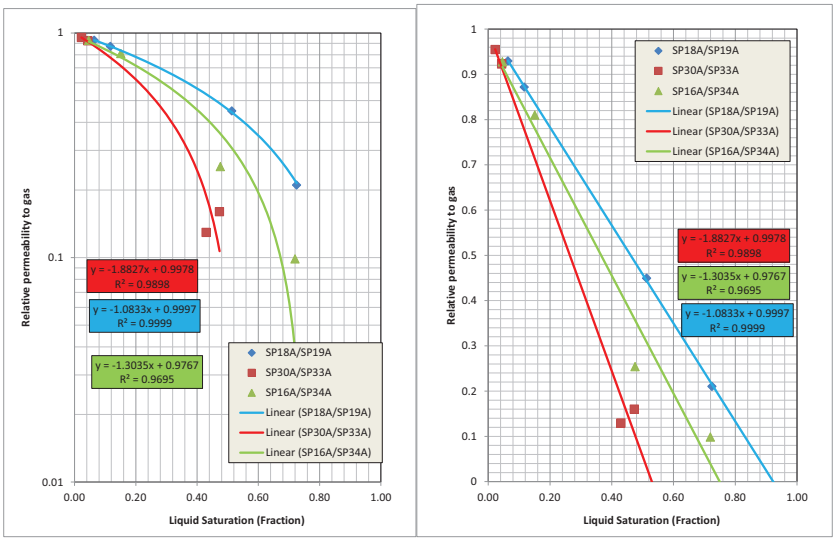

Figure 6: Gas Relative Permeability with Liquid Saturation for Each Core

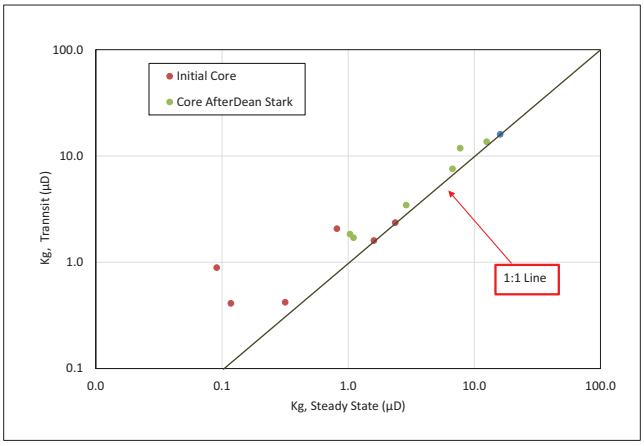

Figure 7: Comparison of Gas Permeability of Steady State with Transient Pressure Method

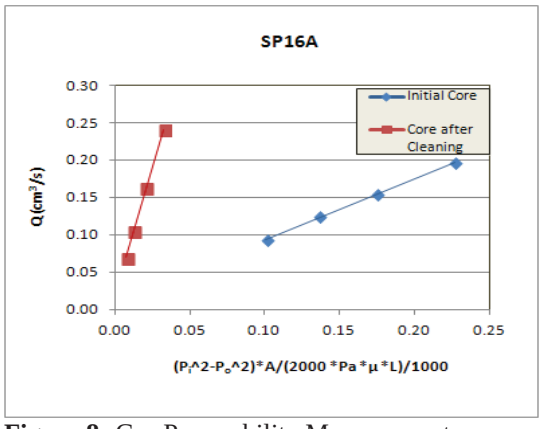

Figure 8: Gas Permeability Measurement Sample

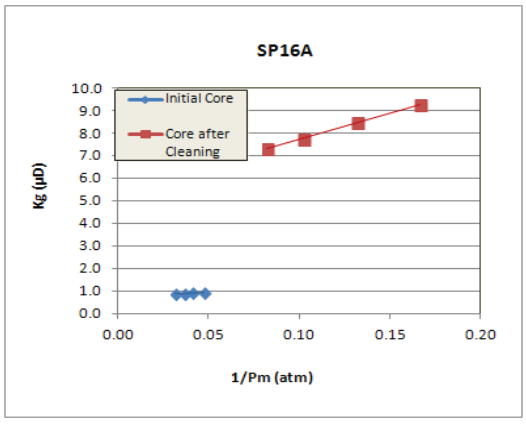

Figure 9: Klinkenberg Correction for Gas Permeability Measurement

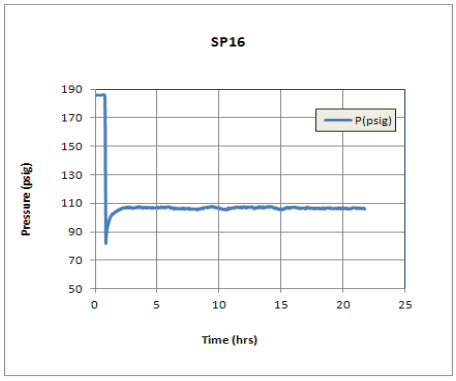

Figure 10: Porosity Measurement with Gas Expansion with Transient Data

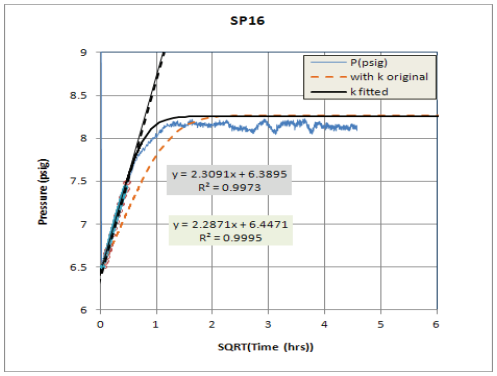

Figure 11: Permeability Calculation from Transient Pressure Data

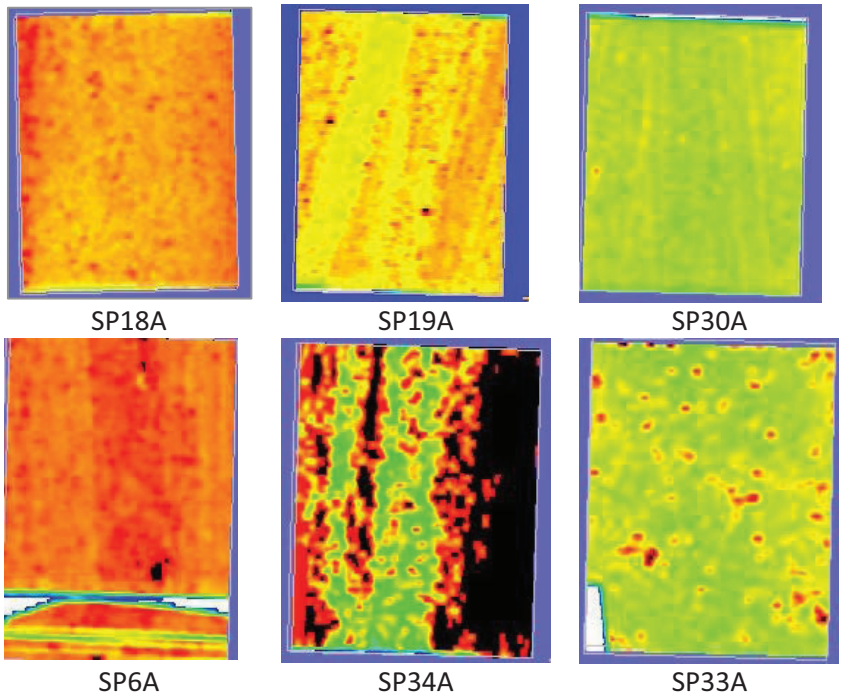

Figure 12: CT image reconstructions of the tested plugs. Plug 6A includes more than one pieces. Plug 34A is the most heterogeneous (tightest) of all samples